IOP Publishing Phys. Scr. 100 (2025) 025401 https://doi.org/10.1088/1402-4896/ada2be

Physica Scripta

PAPER

The effect of state preparation on the probe-bath parameters estimation

Ali Raza Mirza and Jim Al-Khalili

School of Mathematics and Physics, University of Surrey, GU2 7XH, Guildford, United Kingdom

E-mail: a.r.mirza@surrey.ac.uk

Keywords: Spin-spin model, Initial correlations, Parameter Estiamtion, Quantum Fisher information

OPEN ACCESS

RECEIVED
23 September 2024

REVISED
20 November 2024

ACCEPTED FOR PUBLICATION
23 December 2024

PUBLISHED
10 January 2025

Abstract

Projective measurement is a popular method of initial state preparation, which always prepares a pure state. However, in various physical situations of interest, this selective measurement becomes unrealistic. In this paper, we investigate the role of pulsed measurement (a unitary operation) on the estimation of system-environment parameters and compare the estimation results obtained via projective measurement with the results obtained via unitary operation. We argue that in typical situations, parameters can be estimated with higher accuracy if the initial state is prepared with the unitary operator (a pulse). We consider the spin-spin model in which a central two-level system (probe) interacts with a collection of two-level systems (bath). The probe interacts with the bath and attains thermal equilibrium. Then, via unitary operation, the initial state is prepared which evolves unitarily. The properties of the bath are imprinted on the reduced dynamics. Due to the initial probe-bath correlations present in the thermal equilibrium state, an additional factor arises in the dynamics, which has an important role in the parameter estimation. In this paper, we study the estimation of bath temperature and probe-bath coupling strength which is quantified by the quantum Fisher information. Our results are promising as one can improve the precision of the estimates by orders of magnitude (especially in the coupling strength case) via unitary operation and by incorporating the effect of initial correlations.

1. Introduction

Open quantum systems have attracted enormous attention because of their basic role in quantum technologies [1]. Since every quantum system interacts with its environment, leading to decoherence [2, 3]. The study of decoherence enables us to understand how we can harness quantum properties in the development and advancement of modern technologies [4]. One of the important quantum features is to sense information that is not possible with classical physics, known as quantum sensing [5]. The key idea behind this is to utilize a quantum probe (a small controllable quantum system) undergoing decoherence [6]. The use of probes allows us to extract some sensitive information about the environment. There are various theoretical tools available, one of which is to derive analytically the expression for quantum Fisher information (QFI) [7]. This approach not only involves the measurement outcome but also quantifies the precision associated with it [8]. By incorporating the effect of initial correlation (present in the thermal equilibrium state), this precision can be enhanced by an order of magnitude [9]. Since the method of initial state preparation also influences the reduced dynamics, it is interesting to explore the impact of state preparation on the precision of estimates. By using the spin-spin model, we aim to investigate how this affects the quantum Fisher information, and hence the estimation, if the initial state is prepared via unitary operation rather than conventional projective measurement. Additionally, we incorporate the effect of initial correlations to gain further insights.

To learn about the bath parameters such as the probe-bath coupling strength and bath temperature, we first allow our quantum probe to interact with its bath until they both attain an equilibrium state [10]. In due course, a suitable measurement is performed to prepare the probe in the desired initial state. The total probe-bath state

evolves under the action of the total unitary operator. Studying the global probe-bath dynamics is quite challenging due to the large number of degrees of freedom of the bath. One possible way is to use pure dephasing models [11]. However, the drawback is that these models do not tell us anything about the energy exchange between the probe and the bath. Beyond the pure-dephasing, another choice is to use exactly solvable models such as the spin-spin model that considers $z-z$ interaction only [12]. In this paper too, we restrict ourselves to $z-z$ interaction only because other types of system-bath interactions forbid us to solve the model analytically. Once the dynamics are known, a measurement performed on the probe allows us to infer bath properties such as temperature and coupling strength. A convenient parameter estimation approach is to determine quantum Fisher information, which gives ultimate precision in our measurements [13]. According to the quantum Cramér-Rao bound, the variance in any unbiased parameter x is bounded by the reciprocal of the Fisher information [14]. Therefore, to maximize the precision in any estimator x, one has to maximize Fisher information over the interaction time.

To date, many attempts have been made to estimate parameters through quantum estimation theory. It is usual practice to consider the system and environment in a product state at $t=0$. Recent work, such as in [15, 16], shows that the Markovian environment remains in thermal equilibrium and information about the bath is inferred through the quantum correlations established after state preparation. Within the harmonic oscillator bath, the single-qubit quantum probe has been utilized to estimate the cutoff frequency of bath oscillators [17, 18]. Squeezed probes have been subjected to investigation to improve the joint estimation of the nonlinear coupling and of the order of nonlinearity [19]. On the other hand, using quantum resources, the sensitivity of phase estimation has been enhanced [20]. However, these approaches disregard the quantum correlations that existed before the state preparation. Therefore, these findings are questionable, particularly when probe-bath coupling is strong. The initial probe-bath correlations present at thermal equilibrium have been extensively studied [12, 21–24]. More recently, the impact of these correlations in the parameter estimation via the Fisher information approach has also been studied [25–27]. Taking the basic seed of this idea, we extend it to explore the effect of initial correlations in a spin environment and the effect of state preparation. As the state preparation process also influences the system dynamics, thus we aim to investigate the impact of the state preparation on the parameter estimation. The state preparation method used in this paper also incorporates the evolution of the z component of the Bloch vector (n_z), whereas in the case of projective measurement, $n_z=0$ in the initial state and hence in the ensuing dynamics. This non-zero contribution of z component of the Bloch vector affects the evolution and hence the parameter estimation in return. Having a probe-bath thermal equilibrium state at hand, we start our analysis by preparing the probe's initial state via a unitary operation (a pulse). Then we work out the reduced dynamics of our probe. This would be essentially a 2×2 matrix which encapsulates the effect of unitary operation made to prepare the initial state, decoherence, and the initial correlations. In order to derive the expression for quantum Fisher information, we diagonalize this matrix and obtain eigenvalues and eigenvectors. The obtained Fisher information will be a function of the probe-bath interaction time and the estimator (temperature and coupling strength here). Then our goal is to optimize it over the interaction time such that QFI is maximised. It is ideal to obtain explicit expression of QFI for estimating temperature T and coupling g to get intuitive understanding of results. However due to the complexity of analytical expressions of associated partial derivatives, we calculate them numerically. Using the expression of QFI, we quantitatively show that initial correlations and state preparation can be manipulated to improve the accuracy of our measurements.

This paper is organized as follows: In section 2, we model our quantum probe and bath with a paradigmatic spin-spin model and determine the eigenstates. Then, in section 3, we present the scheme of state preparations and the ensuing dynamics both with and without initial correlations. In section 4, we derive analytically an expression for quantum Fisher information and use it to estimate temperature (in 4.2) and probe-bath coupling strength (in 4.3). Finally, we summarize our results in the section 5.

2. Spin-spin model

We consider a single spin-half quantum system (probe) interacting with a group of spin-half quantum systems (bath). The total Hamiltonian can be written as

$$H_{\rm tot}=\begin{cases} H_{S0}+H_B+H_{SB} & t\leqslant 0,\\ H_S+H_B+H_{SB} & t>0,\end{cases} \tag{1}$$

where H_{S0} is the system Hamiltonian before the system state preparation, with the parameters in H_{S0} chosen to aid the state preparation process. H_B is the bath Hamiltonian alone, and H_{SB} is the system-bath interaction Hamiltonian. At $t=0$, we prepare the initial state of our probe, and the system Hamiltonian becomes H_S corresponding to its coherent evolution. Note that H_{S0} is similar to H_S in the sense that both operators live in the

same Hilbert space, but they may have different parameters. Within the spin-spin model, for N spin-half systems in the bath, we have (with $\hbar = 1$)

$$H_{S0} = \frac{\varepsilon_0}{2}\sigma_z + \frac{\Delta}{2}\sigma_x;\ H_S = \frac{\varepsilon}{2}\sigma_z + \frac{\Delta}{2}\sigma_x, \tag{2a}$$

$$H_B = \sum_{i=1}^{N}\left(\frac{\omega_i}{2}\sigma_z^{(i)} + \chi_i\sigma_z^{(i)}\sigma_z^{(i+1)}\right), \tag{2b}$$

$$H_{SB} = \frac{1}{2}\sigma_z \otimes g\sum_{i=1}^{N}\sigma_z^{(i)}. \tag{2c}$$

Here $\sigma_{x,y,z}$ are the Pauli spin operators, ε_0 and ε denote the energy-level spacing of the central spin system before and after the state preparation respectively, Δ is the tunneling amplitude, and ω_i denotes the energy level spacing for the i^{th} spin in the bath. Bath spins interacts with each other via $\sum_{i=1}^{N}\chi_i\sigma_z^{(i)}\sigma_z^{(i+1)}$, where χ_i denotes the inter-spins interaction strength. Our probe interacts with the bath through interaction Hamiltonian H_{SB}, with g as the probe-bath coupling strength. Note that our system Hamiltonian H_S does not commute with the total Hamiltonian, meaning that the system energy is not conserved. Our primary goal is to determine the dynamics of the probe. We express the interaction Hamiltonian into the system and bath operators as $H_{SB} = S \otimes B$, where S is a system operator and B is a bath operator. The states $|n\rangle = |n_1\rangle|n_2\rangle|n_3\rangle...|n_N\rangle$ are the eigenstates of B, with $n_i = 0, 1$ denoting the spin-up and spin-down states with respect to the z axis, respectively. We then have a set of eigenvalue equations

$$g\sum_{i=1}^{N}\sigma_z^{(i)}|n\rangle = G_n|n\rangle;\quad \sum_{i=1}^{N}\omega_i\sigma_z^{(i)}|n\rangle = \Omega_n|n\rangle;\quad \sum_{i=1}^{N}\chi_i\sigma_z^{(i)}\sigma_z^{(i+1)}|n\rangle = \alpha_n|n\rangle; \tag{3}$$

where $G_n = \sum_{i=1}^{N}(-1)^{n_i}g$, $\Omega_n = \sum_{i=1}^{N}(-1)^{n_i}\omega_i$, and $\alpha_n = \sum_{i=1}^{N}\chi_i(-1)^{n_i}(-1)^{n_{i+1}}$ are the eigenvalues of their respective operators. We also assume all environmental spins are coupled to the central spin with equal strength, g.

3. Initial state preparation and dynamics

Here we show analytical details of the initial state preparation process for both the with and without initial correlations cases. Then we show the calculations of the unitary operator and the evolution of both forms of initial states described below.

3.1. Without initial correlations

We first discuss the preparation of the probe's initial state while correlations are ignored. In such a case, the probe and bath are initially in product state $\rho = \rho_{S0} \otimes \rho_B$, with $\rho_{S0} = e^{-\beta H_{S0}}/Z_{S0}$ and $\rho_B = e^{-\beta H_B}/Z_B$ with the partition functions $Z_{S0} = \text{Tr}_S\{e^{-\beta H_{S0}}\}$ and $Z_B = \text{Tr}_B\{e^{-\beta H_B}\}$, where $\beta = 1/k_BT$. Note that this probe-bath state is only justified if the probe-bath interaction is weak enough. Under the condition when $\varepsilon_0 \gg \Delta$, the probe state can be proven to be approximately 'down' along the z-axis. Then, we make a suitable unitary operation to prepare the initial state. For instance, if the desired probe's state is 'up' along the x-axis, then an operator $R = e^{i\frac{\pi}{4}\sigma_y}$, realized by the application of a suitable control pulse, is implemented to the probe. The pulse duration is assumed to be sufficiently smaller than the effective Rabi frequency $\sqrt{\varepsilon_0^2 + \Delta^2}$. After the pulse operation, we have

$$\tilde{\rho}_{\text{tot}} = \tilde{\rho}_{S0} \otimes \rho_B \tag{4}$$

with $\tilde{\rho}_{S0} = e^{-\beta\widetilde{H}_{S0}}/Z_{S0}$ and $\widetilde{H}_{S0} = RH_{S0}R^\dagger$. The action of the pulse is represented by the 'tilde' overhead the operators. Note that we can change the probe's parameters as needed after the state preparation. Doing so, the tunneling term $(\frac{\Delta}{2}\sigma_x)$ contributes significantly. Here, we assume the energy level spacing changes $(\varepsilon_0 \to \varepsilon)$ within a very short time. The probe's initial state can obtained by performing a trace over the bath, where the superscript 'u' represents the 'uncorrelated initial state' as we are ignoring the probe-bath interaction,

$$\rho_{S0}^u = \frac{1}{Z_{S0}}\left\{\mathbb{1}\cosh(\beta\eta_0) - \frac{\sinh(\beta\eta_0)}{\eta_0}\widetilde{H}_{S0}\right\},$$

with $\eta_0 = (1/2)\sqrt{\varepsilon_0^2 + \Delta^2}$. It is useful to write this state in terms of components of the Bloch vector corresponding to this state

$$\begin{pmatrix} n_x^u(0) \\ n_y^u(0) \\ n_z^u(0) \end{pmatrix} = \frac{\sinh(\beta\eta_0)}{Z_{S0}\eta_0}\begin{pmatrix} \varepsilon_0 \\ 0 \\ -\Delta \end{pmatrix}. \tag{5}$$

In order to make further progress, we need to determine the reduced dynamics, which first necessitate the calculation of the total time evolution unitary operator. This operator can be written as $U(t) = \sum_n U_n(t)|n\rangle\langle n|$, where $U_n(t) = e^{-i\frac{\Omega_n}{2}t}e^{-i\alpha_n t}e^{-iH_S^n t}$, which only acts on the system's Hilbert space. Here, $H_S^n \equiv \frac{\xi_n}{2}\sigma_z + \frac{\Delta}{2}\sigma_x$ is the shifted Hamiltonian due to the environmental interaction with the new energy parameter $\xi_n = G_n + \varepsilon$. Now, we can determine the reduced density matrix, $\rho_u(t) = \mathrm{Tr}_B[U(t)\rho^u\,\mathrm{tot}(0)\,U^\dagger(t)]$. After some algebraic manipulations, we obtain

$$\rho_u(t) = \frac{1}{2}\begin{pmatrix} 1 + n_z^u(t) & e^{-\Gamma_u(t)}e^{-i\Omega_u(t)} \\ e^{-\Gamma_u(t)}e^{i\Omega_u(t)} & 1 - n_z^u(t) \end{pmatrix}, \tag{6}$$

where $\Omega_u(t) = \arctan\left[\frac{n_y^u(t)}{n_x^u(t)}\right]$, and the decoherence rate $\Gamma_u(t) = -\frac{1}{2}\ln\{n_x^u(t)\}^2 + \{n_y^u(t)\}^2$. Now, the evolution of the Bloch vector components can be written in general form as $n_i^u(t) = \Theta_{ix}^u(t)n_i^u(0)$ with $i = x, y, z$, and the propagators

$$\Theta_{xx}^u(t) = \sum_n \frac{c_n}{4Z_B\eta_n^2}\{\Delta^2 + \eta_n^2\cos(2\eta_n t)\}, \quad \Theta_{yx}^u(t) = \sum_n \frac{c_n\varepsilon_n}{2Z_B\eta_n}\sin(2\eta_n t), \quad \Theta_{zx}^u(t) = \sum_n \frac{c_n\xi_n\Delta}{2Z_B\eta_n^2}\sin^2(\eta_n t). \tag{7}$$

where $c_n = e^{-\beta(\frac{\Omega_n}{2}+\alpha_n)}$, $Z_B = \sum_n c_n$. For convenience, we work in dimensionless units where every energy parameter is expressed in terms of ε. We have also set $\hbar = k_B = 1$ throughout.

3.2. With initial correlations

In general, our probe-bath state is a correlated state as the probe has interacted with the bath before. To consider a correlated initial state, we assume that our probe has interacted with the bath to achieve a thermal equilibrium state; the Gibbs state $\rho_{\mathrm{th}} = e^{-\beta H}/Z_{\mathrm{tot}}$, since $[H_S, H_{SE}] \neq 0$ and such a state can not be written as a product state. We apply the same pulse that was used in the previous case to prepare the probe state. As a result, we have the correlated probe-bath state (the superscript 'c' stands for 'correlated state')

$$\rho_{\mathrm{tot}}^c(0) = \frac{1}{Z_{\mathrm{tot}}}e^{-\beta(\widetilde{H}_{S0}+H_B+\widetilde{H}_{SB})}, \tag{8}$$

where $Z_{\mathrm{tot}} = \mathrm{Tr}_{SB}\{e^{-\beta(\widetilde{H}_{S0}+H_B+\widetilde{H}_{SB})}\}$ is the total partition function for the combined probe + bath system, and $\widetilde{H}_{SB} = RH_{SB}R^\dagger$. Note that if the probe-bath interaction is sufficiently weak, this state would approximate the product state given in equation (4). Looking at equation (3), we can write $e^{-\beta H_B}|n\rangle = c_n|n\rangle$. Also,

$$(\widetilde{H}_{S0} + \widetilde{H}_{SB})|n\rangle = \left(\frac{\varepsilon_0^n}{2}\sigma_z - \frac{\Delta}{2}\sigma_x\right)|n\rangle \equiv H_{S0}^n|n\rangle,$$

where H_{S0}^n is a 'shifted' system Hamiltonian with a new energy parameter $\varepsilon_0^n = G_n + \varepsilon_0$. In this case, the Bloch vector components are

$$\begin{pmatrix} n_x^c(0) \\ n_y^c(0) \\ n_z^c(0) \end{pmatrix} = \sum_n \frac{c_n\sinh(\beta\eta_0^n)}{Z_{\mathrm{tot}}\eta_0^n}\begin{pmatrix} \varepsilon_0^n \\ 0 \\ -\Delta \end{pmatrix}, \tag{9}$$

where $\eta_0^n = (1/2)\sqrt{(\varepsilon_0^n)^2 + \Delta^2}$ under the action of unitary operator. Our probe-bath correlated initial state evolves and the reduced density matrix is

$$\rho_c(t) = \frac{1}{Z\mathrm{tot}}\sum_n J_n^{\mathrm{corr}}c_n U_n(t)|\psi\rangle\langle\psi|\,U_n^\dagger(t), = \frac{1}{2}\begin{pmatrix} 1 + n_z^c(t) & e^{-\Gamma_c(t)}e^{-i\Omega_c(t)} \\ e^{-\Gamma_c(t)}e^{i\Omega_c(t)} & 1 - n_z^c(t) \end{pmatrix}, \tag{10}$$

where $Z\mathrm{tot} = \sum_n J_n^{\mathrm{corr}}c_n$, $J_n^{\mathrm{corr}} = 2\cosh(\beta\eta_n)$, $\eta_n = (1/2)\sqrt{\xi_n^2 + \Delta^2}$, $\Omega_c(t) = \arctan\left[\frac{n_y^c(t)}{n_x^c(t)}\right]$, and the decoherence rate $\Gamma_c(t) = -\frac{1}{2}\ln\{n_x^c(t)\}^2 + \{n_y^c(t)\}^2$. The evolution of the corresponding Bloch vector components can be expressed in general form as $n_i^c(t) = \Theta_{ix}^c(t)n_i^c(0)$ with $i = x, y, z$. The propagators $\Theta_{ix}^c(t)$ are given as

$$\Theta_{xx}^c(t) = \sum_n \frac{J_n^{\mathrm{corr}}c_n}{4Z_{\mathrm{tot}}\eta_n^2}\{\Delta^2 + \eta_n^2\cos(2\eta_n t)\}; \quad \Theta_{yx}^c(t) = \sum_n \frac{J_n^{\mathrm{corr}}c_n\varepsilon_n}{2Z_{\mathrm{tot}}\eta_n}\sin(2\eta_n t); \quad \Theta_{zx}^c(t) = \sum_n \frac{J_n^{\mathrm{corr}}c_n\xi_n\Delta}{2Z_{\mathrm{tot}}\eta_n^2}\sin^2(\eta_n t). \tag{11}$$

If we compare these propagators with those given in (7), we see that $1/Z_B \rightarrow J_n^{\rm corr}/Z$ tot, which essentially captures the effect of initial correlations.

4. Parameter estimation

The quantum Fisher information is related to the Cramer–Rao bound; the larger the QFI, the greater the precision in our estimate. In this section, we first derive the formula for quantum Fisher information for our probe. We then present estimation results in the subsequent sections.

4.1. Quantum fisher information

To quantify the precision with which a general environment parameter x (in our case this is temperature, T, or the coupling strength, g) can be estimated, we use quantum Fisher information, which is defined by [17]

$$F(x) = \sum_{n=1}^{2} \frac{(\rho'_n)^2}{\rho_n} + 2\sum_{n\neq m} \frac{(\rho_n - \rho_m)^2}{\rho_n + \rho_m} \langle v_m | v'_n \rangle^2, \tag{12}$$

where $\rho_{m,n}$ and $v_{m,n}$ being eigenvalues and eigenvectors of any density matrix, respectively. The prime superscript denotes the derivative with-respect-to the estimator x. Thus, the first task is to diagonalize matrices in equations (6) and (10). The eigenvalues of equation (10) are $\rho_1^c(t) = \frac{1}{2}[1 + \mathcal{N}_c(t)]$, $\rho_2^c(t) = \frac{1}{2}[1 - \mathcal{N}_c(t)]$ with $\mathcal{N}_c(t) = \sqrt{\{n_x^c(t)\}^2 + \{n_y^c(t)\}^2 + \{n_z^c(t)\}^2}$. And the corresponding eigenvectors are

$$|v_1^c\rangle = \sqrt{\frac{\mathcal{N}_c + n_z^c}{2\mathcal{N}_c}}\ |\downarrow\rangle_z - e^{-i\Omega_c}\sqrt{\frac{\mathcal{N}_c - n_z^c}{2\mathcal{N}_c}}\ |\uparrow\rangle_z; \qquad |v_2^c\rangle = \sqrt{\frac{\mathcal{N}_c - n_z^c}{2\mathcal{N}_c}}\ |\downarrow\rangle_z + e^{-i\Omega_c}\sqrt{\frac{\mathcal{N}_c + n_z^c}{2\mathcal{N}_c}}\ |\uparrow\rangle_z, \tag{13}$$

where $|\uparrow\rangle_z$ and $|\downarrow\rangle_z$ are eigenstates of σ_z with eigenvalues $+1$ and -1, respectively. If we disregard initial correlations, we obtain a similar set of eigenvalues and eigenvectors, but having superscript 'u' with $J_n^{\rm corr} = 1$. Now we are equipped to write the final expression of quantum Fisher information, taking initial correlations into account. We have

$$F_c = \frac{(\Gamma'_c - n_z^c(n_z^c)' e^{2\Gamma_c})^2}{f_c(e^{2\Gamma_c} - f_c)} + \frac{((n_z^c)' + n_z^c \Gamma'_c)^2}{f_c} + \frac{(\chi'_c)^2}{e^{2\Gamma_c}}, \tag{14}$$

with $f_c = 1 + (n_z^c)^2 e^{2\Gamma_c}$. In the chosen model, both diagonal and off-diagonal entries evolve. Therefore, we can see the Fisher information also depends on the time-dependent factor n_z^c, unlike the pure-dephasing case where only off-diagonal entries evolve. If we set $n_z^c = 0$, implying $f_c = 1$, we recover the Fisher information given in [8], which benchmarks our calculations. If initial correlations are discarded, the QFI is

$$F_u = \frac{(\Gamma'_u - n_z^u(n_z^u)' e^{2\Gamma_u})^2}{f_u(e^{2\Gamma_u} - f_u)} + \frac{((n_z^u)' + n_z^u \Gamma'_u)^2}{f_u} + \frac{(\chi'_u)^2}{e^{2\Gamma_u}}, \tag{15}$$

with $f_u = 1 + (n_z^u)^2 e^{2\Gamma_u}$.

4.2. Estimating environment temperature

Having all these analytics at hand, we can move to the main part of this paper, which relies on the results of estimation. Recall that our primary goal is to investigate the role of initial correlations and state preparation to look for maximum Fisher information. Our QFI is a function of time, temperature and probe-bath coupling strength. To estimate bath temperature with ultimate precision, we need to find the interaction time at which QFI is maximum. To proceed, we first need to calculate partial derivatives with-respect-to temperature, T, and use them in equations (14) and (15). The effect of correlations is encapsulated by the factor $J_n^{\rm corr}$ appearing in the propagators, $\Theta_{ix}^c(t)$. Firstly, we consider the probe-bath coupling to be weak, so the effect of correlations is expected to be less [21, 25, 28], which in turn has a negligible impact on the accuracy.

Figure 1(a) shows the behavior of quantum Fisher information as a function of time at various temperatures. The solid curves signify QFI taking initial correlations into account, whereas dotted curves discard the effect of correlations. Peak values represent the optimized QFI, which is in turn the ultimate precision in the temperature estimation. For simplicity, we first consider non-interacting ($\chi = 0$) spins in the bath (with $N = 50$). We see that the effect of the initial correlation is almost negligible, as the coupling strength is very small ($g = 0.01$). Next, we notice that the peak is maximum at lower temperatures, which means the low temperature is favorable for better estimation. As the temperature is raised, the decoherence process speeds up and the precision drops. We next compare our results with those results of [27], where the initial state was prepared via the usual projective measurement. Under the same set of probe-bath parameters as in figure 1(a), we show the behavior of optimized quantum Fisher information as a function of temperature T, for the case if the initial state is prepared via

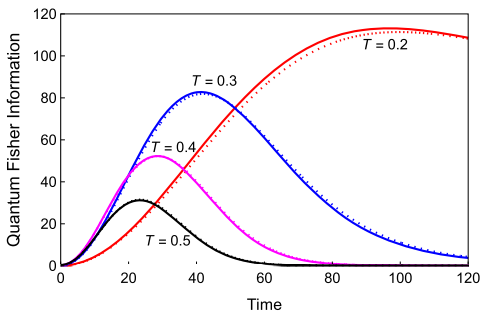

(a) The behavior of QFI as a function of time while estimating temperature. Solid curves include the correlations' effect whereas dotted ones ignore this effect.

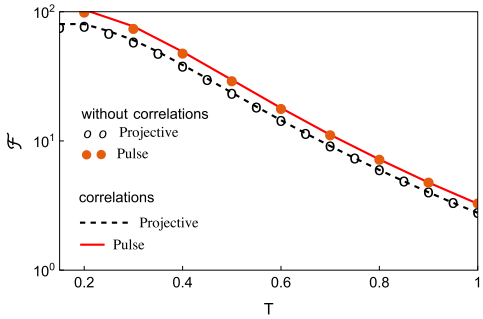

(b) The behavior of optimized QFI, that is, $\mathcal{F}$ estimating temperature T. Solid-red & dotted black curves include the correlations' whereas other ones ignore this effect.

Figure 1. The number of environmental spins is $N = 50$, coupling strength $g = 0.01$, and inter-spin interaction $\chi = 0$. The rest of probe-bath parameters are $\omega_i = 1, \varepsilon_0 = 4, \varepsilon = 2$ and $\Delta = 1$.

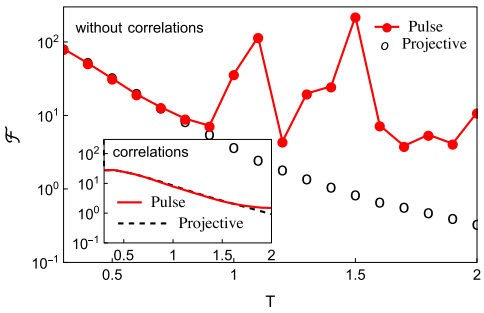

(a) (Color online) Same as Fig. 1a except that the interaction strength is stronger, that is $g = 1$.

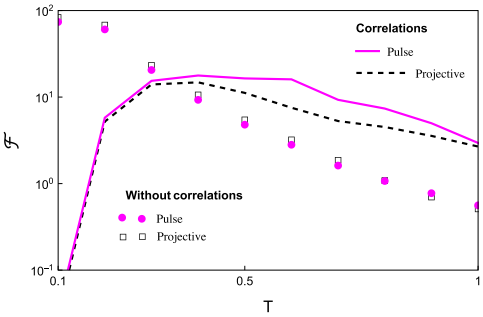

(b) (Color online) The role of inter-spin interaction $\chi = 0.1$ with $N = 10$. Rest is the same as Fig. 1a

Figure 2. The behaviour of optimized QFI (with and without initial correlations) as a function of temperature for projective measurement and unitary operation.

projective measurement (call it $\mathcal{F}_{\text{proj}}$ in black-dashed), versus $\mathcal{F}_{\text{pulse}}$ (in red-solid if the initial state is prepared via unitary operator) in figure 1(b). We notice that $\mathcal{F}_{\text{pulse}}$ is slightly higher than $\mathcal{F}_{\text{proj}}$ if initial correlations are incorporated. We repeat this for both cases but without initial correlations using equation (15). The same behavior is seen as solid circles (pulse) and empty circles (projective) overlap with their respective curves of correlations. The reason for this is that, within a weak coupling regime, the correlation energy is dominated by the thermal energy β [27]. However, if coupling strength increased to $g = 1$, the difference between $\mathcal{F}_{\text{pulse}}$ and $\mathcal{F}_{\text{proj}}$ is amplified if we discard initial correlations. As shown in figure 2(a), $\mathcal{F}_{\text{pulse}}$ (solid-circled-red) is greater than $\mathcal{F}_{\text{proj}}$ (black-empty circles) for higher values of the temperature, which is what expected. Note that the Bloch vector components given in equations (5) and (9) depend explicitly on temperature. As temperature increases, the orientation of the initial state changes. That is, the x and y components of the Bloch vector decrease in magnitude and, as a result, the degree of mixedness increases. This improves the precision of temperature estimation by an order of magnitude. However, if we take the initial correlations into account, $\mathcal{F}_{\text{pulse}}$ (solid-red) and $\mathcal{F}_{\text{proj}}$ (dashed-black) almost overlap as shown in the inset of figure. This is because the thermal energy and interaction energy are equally dominant and the effect of state preparation almost disappears. As a final comment, at higher temperatures, pulsed measurement is favorable since it gives the greatest accuracy.

Next, we investigate the impact of inter-spin interaction $\chi = 0.1$. With a small number of bath spins, the decoherence process slows down. As a result, initial correlations and the role of state preparation can be better realized. Results are shown in figure 2(b) with a smaller bath of $N = 10$. Figure 2(b) compares the behavior of $\mathcal{F}_{\text{pulse}}$ (solid-magenta) versus $\mathcal{F}_{\text{proj}}$ (dashed-black), if correlations are considered. One can clearly see that pulsed measurement made at $t = 0$, produces larger QFI than is QFI achievable with projective measurement. On the other hand, in the uncorrelated cases, no appreciable role of state preparation is seen. In the smaller spin bath, we expected more Fisher information than in the larger bath. However, we notice that $\mathcal{F}_{\text{pulse}}$ with $N = 10$

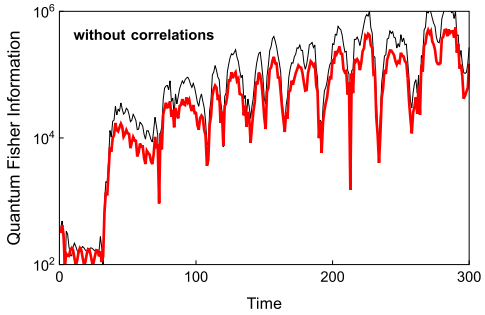

(a) Coupling strength $g = 0.1$, and bath temperature $T = 1$.

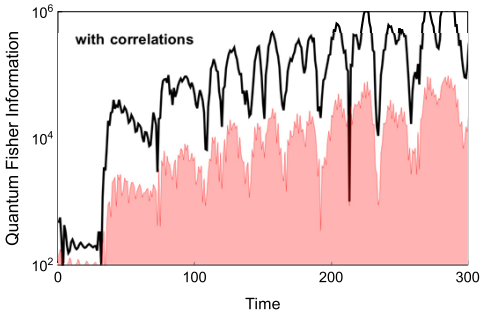

(b) Same as Fig. 3a except that now we have incorporated the effect of initial correlations.

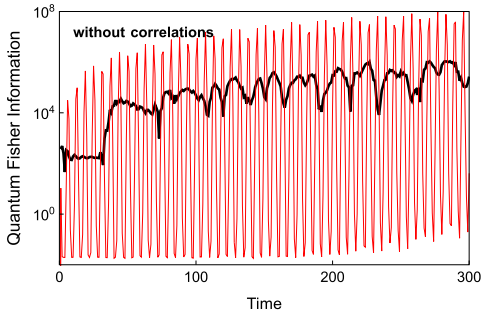

(c) Coupling strength $g = 0.5$, and bath temperature $T = 0.5$.

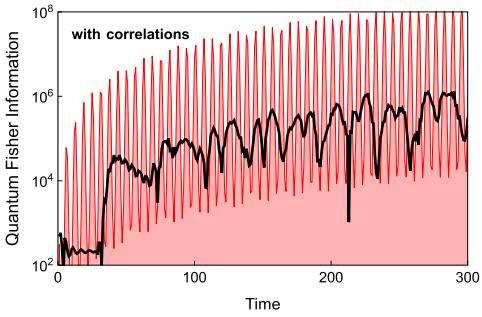

(d) Same as Fig. 3c except that now we have incorporated the effect of initial correlations.

Figure 3. The behavior of quantum Fisher information with pulsed (red) versus projective measurement (black) while estimating probe-bath coupling strength. Probe-bath parameters other than in figures 3(a) and 3(c) are the same as in figure 1(a).

in figure 2(b) is less than $\mathscr{F}_{\text{pulse}}$ with $N = 50$ (figure 2(a)). This means that inter-spin interactions play a significantly negative role in precision improvement as $\mathscr{F}_{\text{pulse}}$ has been suppressed in figure 2(b). Let us explain this situation. Three key factors control the orientation of environment spins, which are; energy biases ω_i, probe-bath coupling strength g, and the inter-spin interaction χ_i. Consider, $\chi_i > 0$, that is, the interaction between environment spins is anti-ferromagnetic. Now, positive values of g and ω_i will tend to align the environment spins (ferromagnetic) while $\chi_i > 0$ will tend to anti-align them. Thus by choosing the appropriate values of g and ω_i, we can minimise the inter-spin interaction. By doing so, we can improve the accuracy. The incorporation of inter-spin interaction prohibits us from considering the higher number of environment spins as it makes the numerical solution challenging. Thus, we limit ourselves to considering $N = 10$ to study the effect of inter-spin interaction.

4.3. Estimating probe-bath coupling strength

Next, we consider the impact of state preparation on the estimation of coupling strength. Again, we consider equation (14) and equation (15), but this time we require derivatives with-respect-to coupling strength g.

The results are illustrated in figure 3(a), where we have shown the QFI as a function of interaction time, keeping temperature and coupling strength fixed at $T = 1$ and $g = 0.1$, respectively. The red-solid curves denotes $\text{QFI}_{\text{pulse}}$ whereas the black curves signify QFI_{proj}. At least two comments can be made regarding this result. First, the quantum Fisher information continues to increase as a function of time, unlike in the case of coupling strength estimation where we see peaks, as in figure 1(a). The source of this continuous increase is the derivatives $\frac{\partial}{\partial_g}\Gamma$, $\frac{\partial}{\partial_g}\Omega$ and $\frac{\partial}{\partial_g}n_z$, which oscillate very fast in the long time limit. Therefore, our measurement result becomes extremely sensitive to the coupling strength g. Consequently, the interaction time is determined by the level of accuracy needed. The same behaviour has been seen in the [29]. Secondly, if we ignore correlations, $\text{QFI}_{\text{proj}} > \text{QFI}_{\text{pulse}}$ always. A similar trend is seen if we incorporate the effect of correlations as shown in figure 3(b). This means that at higher temperatures while estimating the coupling strength, the projective measurement method is favoured over the pulsed one under consideration. However, the situation changes if we jump to the low-temperature regime. Figure 3(c) depicts the behaviour of quantum Fisher information as a function of time at a fixed value of temperature ($T = 0.5$) and coupling strength ($g = 0.5$). Here now we see the mixed behaviour of QFI as one can see $\text{QFI}_{\text{pulse}} > \text{QFI}_{\text{proj}}$ at certain times and converse at the rest of times, in either with (Figure 3(d)) or without (figure 3(c)) correlation case. The objective of our work is once again quite

clear as one can see that higher accuracy can be obtained if pulsed measurement is performed rather than projective.

5. Conclusion

Initial correlations and pulsed measurement are the two basic elements in our analysis and decoherence is a challenge in both cases. We considered a variety of physical situations and investigated how to obtain the best estimates using a quantum probe. Our study reveals that how we choose to engineer the bath or choose the temperature is crucial in order to keep the error in our measurement minimal. Results presented in this paper show that the role of initial state preparation and initial correlations can be very significant, especially in the strong coupling regime and at low temperatures. This has important implications for quantum sensing since one can obtain high ultimate precision in the estimates via pulsed measurement and by incorporating the effect of initial correlations.

Acknowledgments

A. R. Mirza and J. Al-Khalili are grateful for support under grant no. RN0491A from the John Templeton Foundation Trust.

Data availability statement

All data that support the findings of this study are included within the article (and any supplementary files).

ORCID iDs

Ali Raza Mirza https://orcid.org/0000-0002-8532-7699

References

[1] Haroche S, Raimond J-M and Dowling J P 2014 Exploring the quantum: atoms, cavities, and photons *American Journal of Physics* **82** 86–7
[2] Schlosshauer M A 2007 *Decoherence: and the quantum-to-classical transition* (Springer Science & Business Media)
[3] Breuer H-P *et al* 2002 *The theory of open quantum systems* (Oxford University Press on Demand)
[4] Schleich W P *et al* 2016 Quantum technology: from research to application *Applied Physics* B **122** 1–31
[5] Degen C L, Reinhard F and Cappellaro P 2017 Quantum sensing *Reviews of modern physics* **89** 035002
[6] Benedetti C, Buscemi F, Bordone P and Paris M G 2014 Quantum probes for the spectral properties of a classical environment *Physical Review* A **89** 032114
[7] Petz D and Ghinea C 2011 Introduction to quantum fisher information *In Quantum probability and related topics* 261–81(World Scientific)
[8] Ather H and Chaudhry A Z 2021 Improving the estimation of environment parameters via initial probe-environment correlations *Physical Review* A **104** 012211
[9] Mirza A R and Chaudhry A Z 2024 Improving the estimation of environment parameters via a two-qubit scheme *Scientific Reports* **14** 6803
[10] Mirza A R, Zia M and Chaudhry A Z 2021 Master equation incorporating the system-environment correlations present in the joint equilibrium state *Physical Review* A **104** 042205
[11] Morozov V, Mathey S and Röpke G 2012 Decoherence in an exactly solvable qubit model with initial qubit-environment correlations *Physical Review* A **85** 022101
[12] Majeed M and Chaudhry A Z 2019 Effect of initial system-environment correlations with spin environments *The European Physical Journal* D **73** 1–11
[13] Chaudhry A Z 2015 Detecting the presence of weak magnetic fields using nitrogen-vacancy centers *Physical Review* A **91** 062111
[14] Rao C R 2008 Cramér-rao bound *Scholarpedia* **3** 6533
[15] Wu W and Shi C 2020 Quantum parameter estimation in a dissipative environment *Physical Review* A **102** 032607
[16] Tamascelli D, Benedetti C, Breuer H-P and Paris M G 2020 Quantum probing beyond pure dephasing *New Journal of Physics* **22** 083027
[17] Benedetti C, Sehdaran F S, Zandi M H and Paris M G 2018 Quantum probes for the cutoff frequency of ohmic environments *Physical Review* A **97** 012126
[18] Benedetti C and Paris M G 2014 Characterization of classical gaussian processes using quantum probes *Physics Letters A* **378** 2495–500
[19] Candeloro A *et al* 2021 Quantum probes for the characterization of nonlinear media *Entropy* **23** 1353
[20] Ciampini M A *et al* 2016 Quantum-enhanced multiparameter estimation in multiarm interferometers *Scientific reports* **6** 28881
[21] Chaudhry A Z and Gong J 2013 Role of initial system-environment correlations: A master equation approach *Physical Review* A **88** 052107
[22] Chaudhry A Z and Gong J 2014 The effect of state preparation in a many-body system *Canadian Journal of Chemistry* **92** 119–27
[23] Zhang Y-J, Han W, Xia Y-J, Yu Y-M and Fan H 2015 Role of initial system-bath correlation on coherence trapping *Scientific reports* **5** 1–9

[24] Chen C-C and Goan H-S 2016 Effects of initial system-environment correlations on open-quantum-system dynamics and state preparation *Physical Review* A **93** 032113
[25] Mirza A R, Jamil M N and Chaudhry A Z 2024 The role of initial system-environment correlations with a spin environment *International Journal of Modern Physics* B 2450429
[26] Zhang C and Gong B 2024 Improving the accuracies of estimating environment parameters via initial probe-environment correlations *Physica Scripta* **99** 025101
[27] Mirza A R and Al-Khalili J 2024 The impact of quantum correlations on parameter estimation in a spin reservoir *Physica Scripta* (https://doi.org/10.1088/1402-4896/ad7f11)
[28] Mirza A R 2023 *Improving the understanding of the dynamics of open quantum systems* arXiv:2402.10901
[29] Mirza A R and Al-Khalili J 2024 *The role of initial system-environment correlations in the accuracies of parameters within spin-spin model* arXiv:2407.03584